Original Paper

Cellular Physiology and Biochemistry

Cell Physiol Biochem 2010;26:609-618

Accepted: August 17, 2010

# Periplocin Inhibits Growth of Lung Cancer *in vitro* and *in vivo* by Blocking AKT/ERK Signaling Pathways

Ze J. Lu[1], Yan Zhou[1], Qi Song[1], Zhao Qin[2], Hong Zhang[2], Yong J. Zhou[1], Lan T. Gou[1], Jin L. Yang[1] and Feng Luo[1]

[1]State Key Laboratory of Biotherapy and Cancer Center, West China Hospital, Sichuan University, Chengdu, Sichuan Province, [2]Research Institute of Plant Application and Development, Sichuan Normal University, Chengdu

**Key Words**

Lung cancer • Periplocin • Antitumor agent • AKT • ERK

**Abstract**

Periplocin is one of cardenolides isolated from cortex periplocae which is used for treatment of rheumatoid arthritis and reinforcement of bones and tendons in traditional medicine. Here, we investigated the anti-tumor activity of periplocin against lung cancer cells both *in vitro* and *in vivo*, and explored its anti-cancer mechanism. Periplocin inhibited the growth of lung cancer cells and induced their apoptosis in time- and dose-dependent manners by cell cycle arrest in G0/G1 phase. Periplocin exhibited anti-tumor activity both in human (A549) and mouse (LL/2) lung cancer xenograft models. Immunohistochemical analysis revealed that intratumoral angiogenesis was significantly suppressed. Furthermore, anti-cancer activity mediated by periplocin was associated with decreased level of phosphorylated AKT and ERK both *in vitro* and *in vivo*, which were important for cell growth and survival. Moreover, periplocin induced apoptosis by downregulating Bcl-2 and upregulating Bax, leading to activation of caspase-3 and caspase-9. These findings suggested that periplocin could inhibit the growth of lung cancer both *in vitro* and *in vivo*, which could be attributed to the inhibition of proliferation and the induction of apoptosis signaling pathway, such as AKT and ERK. These observations provide further evidence on the anti-tumor effect of periplocin, and it may be of importance to further explore its potential role as a therapeutic agent for cancer.



## Introduction

Lung cancer is the leading cause of cancer-related deaths in the world. Most patients with lung cancer have advanced disease at diagnosis, and are characterized by dismal prognoses with a low five year survival rate [1]. Chemotherapy, including camptothecin, taxane, platin, and vinca alkaloid derivatives, has only a limited effect [2].

KARGER

Fax +41 61 306 12 34
E-Mail karger@karger.ch
www.karger.com


1015-8987/10/0265-0609$26.00/0

Accessible online at:
www.karger.com/cpb

P.H.D. Jin Liang Yang
State Key Laboratory of Biotherapy and Cancer Center
West China Hospital of Sichuan University, Chengdu 610041
Sichuan Province (China)
E-Mail jlyang01@163.com

The large number of cases and poor survival rates under current therapies necessitate the search for novel drugs for lung cancer. Recent researches have shown that plant products exhibited chemopreventive effects [3]. As many as 70% of therapeutic drugs in use are derived from plants. Cardiac glycosides, known as ligands of the sodium pump, have been widely used for the treatment of heart failure. However, epidemiological evaluations and subsequent demonstration of anti-cancer activity *in vitro* and *in vivo* have indicated the possibility of developing this class of compound as chemotherapeutic agents in oncology [4]. The death rate and cancer recurrence turned out to be lower in women with breast cancer treated with digitalis than in non-treated patients [5]. In addition, some cardiotonic steroids, anvirzel and UNBS-1450, are entering phase I clinical trials [6, 7]. Successful anti-cancer drugs can trigger tumor cell death. Most lung cancer cells, however, are naturally resistant to not only apoptosis but also necrosis, autophagy, and senescence, which is caused by autocrined chemoresistant proteins and constitutive activation of cell proliferation signaling pathways [8-10]. Both protein kinase B (AKT) and extracellular signal regulated kinase (ERK) are upregulated in lung cancer cells [11, 12]. Besides, signal transducers and activators of transcription 3 (STAT3) has been widely implicated in a wide variety of human cancers, including lung cancer [13]. Drugs targeting those signaling pathways described above might serve in cancer therapy.

Periplocin is a cardiac glycoside derived from cortex periplocae, but recent studies have shown that periplocin can inhibit the growth of cancer cells (e.g. U937 and PC3 cells) and induce their apoptosis [14]. Up to now, there have been few studies concerning how periplocin can be involved in the regulation of cancer cell proliferation and apoptosis.

In present study, we investigated the anti-tumor activity of periplocin against lung cancer cells and explored its anti-cancer mechanism both *in vitro* and *in vivo*. Besides, both human and mouse (A549 and LL/2) lung cancer xenograft models were established to test whether periplocin could inhibit the growth of lung cancer. Results *in vitro* demonstrated that periplocin inhibited the growth of lung cancer cells and induced their apoptosis, which was related to G0/G1 phase cell cycle arrest. Moreover, periplocin inhibited the growth of lung cancer both in A549 and LL/2 murine models. Furthermore, inhibitory effect of periplocin against lung cancer was associated with decreased level of phosphorylated AKT and ERK *in vitro* and *in vivo*. Our data exhibited that periplocin may be a candidate for the therapy of human lung cancer.

## Materials and Methods

*Reagents and antibodies*

3-(4,5-dimethylthiazol-2-yl)-2,5-diphenyltetrazolium bromide (MTT), dimethyl sulfoxide (DMSO), RNase A and propidium iodide (PI) were purchased from Sigma (St. Louis, MO). DNA marker and protease K were purchased from TaKaRa (Dalian, China). The primary antibodies against AKT/p-AKT, ERK/p-ERK, STAT3/p-STAT3, cyclinD1, caspase-3, caspase-8, caspase-9 and β-actin were acquired from Cell Signaling Technology (Beverly, MA); antibodies against Bcl-2, Bax and CD31 were from Santa Cruz Biotechnology Co. (Santa Cruz, CA). Secondary antibodies were purchased from Zhongshan Biological (Beijing, China). The protein assay kit was purchased from Bio-Rad (Hercules, CA). ECL detection system was from Amersham (Arlington Heights, IL). Periplocin (purity>98%) was provided by Research Institute of Plant Application and Development (Chengdu, China). The periplocin was prepared in normal sodium (NS) at a concentration of 10mg/ml. Drug stock was diluted in RPMI 1640 (containing 10% FBS) when required for assays.

*Tumor cell line and culture*

The human lung cancer cell lines A549, SPCA-1, H1975, NCI-H446, NCI-H460, NCI-H292, NCI-H69 and murine lewis lung cancer cell line LL/2 were obtained from the American Type Culture Collection (ATCC, Manassas, VA). 95D cells were provided by our laboratory. These cells were cultured in RPMI 1640 or DMEM (Life Technologies, Bedford, MA) containing 10% heat-inactivated fatal bovine serum, 100 units/ml penicillin and 100 units/ml streptomycin in a humid chamber at 37°C under 5% $CO_2$ in atmosphere.

*Cell viability assay*

The cell viability of periplocin-treated cancer cells was determined by the MTT assay. Briefly, cells ($4\text{-}5x10^3$) were seeded in 96-well plates and cultured for 24 hours, followed by different concentrations of periplocin (0, 0.0125, 0.025, 0.05, 0.1, 0.2, 0.3 and 0.4μg/ml) treatment for 24, 48, or 72 h. A volume of 10μl of 10mg/ml MTT was added per well and incubated for 2.5 more hours at 37°C, then the supernatant fluid was removed and 150μl of DMSO was added for 15-20 min. The light absorptions (OD) were measured at 570nm with SpectraMAXM5 microplate spectrophotometer (Molecular Devices). All experiments were performed in triplicate. The effect of periplocin on tumor cells viability was expressed by $IC_{50}$ of each cell line. The effect of periplocin on the proliferation of lung cancer cells was expressed by the percentage of cell growth inhibition, with the use of the following formula: Inhibitory rate=([OD control group OD experiment group]/OD control group) x 100%.

*Flow cytometric assay*

The percentage of the apoptotic cells and the cell cycle distribution of periplocin-treated cells were analyzed by Flow cytometry. Briefly, lung cancer cells ($3x10^5$/well) were plated in 6-well plates. After incubation overnight, periplocin was added with different concentrations (0, 0.0125, 0.025, 0.05, 0.1, 0.2, 0.3

**Table 1.** The cytotoxicity effect of periplocin on lung cancer cells. Each cell line was treated with various concentrations of periplocin for 48 h respectively. All the experiments were done thrice in triplicates.

| Tumor cell line | Cell type | $IC_{50}$( μ g/ml ) |
|---|---|---|
| SPCA-1 | Human non-small cell lung cancer cell line | 0.24 |
| A549 | Human non-small cell lung cancer cell line | 0.08 |
| H1975 | Human non-small cell lung cancer cell line | 0.21 |
| 95D | Human non-small cell lung cancer cell line | 0.43 |
| NCI-H460 | Human non-small cell lung cancer cell line | 0.4 |
| NCI-H292 | Human non-small cell lung cancer cell line | 25 |
| NCI-H446 | Human small cell lung cancer cell line | 0.18 |
| NCI-H69 | Human small cell lung cancer cell line | 37 |
| LL/2 | Mouse lung cancer cell line | 0.35 |

and 0.4 μg/ml). After 48 hours, the cells were harvested and resuspended in 1ml of hypotonic fluorochrome solution containing 50μg/ml PI in 0.1% sodium citrate plus 0.1% Triton X-100 and subjected to FCM (ESP Elite, Beckman Coulter, Fullerton, CA) analysis immediately.

*DNA fragmentation*

Apoptotic cells produce characteristic DNA ladders made up of nucleotide fragments which are visualized by staining with ethidium bromide following DNA-agarose gel electrophoresis. We used DNA fragmentation as one of the criteria of cell apoptosis. Briefly, cells were cultured and treated with periplocin as described above. The cells were harvested and fixed in 70% ethanol for 10 min, when more than 50% of them became round. After washed with PBS, the cells were solubilized in 0.1ml of lysis buffer (5mM Tris/HCl [pH 8.0], 0.25% Nonidet P-40 and 1mM EDTA) on ice for 1 h, followed by adding RNase A (200μg/ml) and proteinase K (300μg/ml) at 37°C for 1 more hour. Subsequently, samples were electrophoresised at 50V for 50 to 70 min. Finally, images were captured with the Versa-Doc Imaging System (Bio-Rad).

*Western blot*

Cells were cultured and treated with periplocin as described above. Then cells were cracked in lysis buffer. After centrifuged at 15,000 rpm for 30 min, equal amounts of protein from control cells and treated cells were subjected to electrophoresis in 12% SDS-PAGE. The proteins in gel were electroblotted onto PVDF membranes (Millipore) by wet blotting. After blocked in buffer (1xTBS, 0.1% Tween-20 and 5% w/v dry nonfat milk) at 4°C, membranes were incubated with the desired primary antibody, followed by incubation with appropriate peroxidase-conjugated secondary antibody. Reactive bands were detected by the enhanced chemiluminescence (Amersham Biosciences Corp, Piscataway, NJ).

*Animal tumor models and treatment*

6-8 week old athymic nude mice (SPF grade) and female C57BL/6 mice were purchased from the Laboratory Animal Center of Sichuan University (Chengdu, China). All studies involving mice were approved by the Institutional Animal Care and Use Committee. Athymic nude mice were inoculated with A549 cells ($1.0x10^7$/0.1 ml), while C57BL/6 mice were injected s.c. in the right axillary fossa with LL/2 cells ($1x10^6$/0.1 ml). In preliminary experiments, we had performed a series of experiments in order to determine the optimum doses of periplocin. Five and fifteen days after inoculation, tumors were palpable in C57BL/6 mice and athymic nude mice respectively. Mice were randomly assigned into each group (n=6/group in C57BL/6 mice and n=5/group in athymic nude mice). Treatments were given i.p. with NS, periplocin(50μg), or periplocin(100μg) every day for 14 days respectively. Tumor volumes were estimated by the formula 0.52 x length x $width^2$ in which length and perpendicular width were measured by caliper. Subsequently, tissues were subjected to histologic and immunohistochemical analysis. In a separate survival experiment with other three groups of C57BL/6 mice (n=10 mice/group), survival time of mice was observed to evaluate the life-prolonging effect.

*Immunohistochemistry*

Immunohistochemistry was performed to detect the expression of p-AKT and p-ERK in tumor tissue. Moreover, tumor microvessel density was evaluated. Briefly, paraffin-embedded sections were incubated with Rabbit polyclonal antibodies against p-AKT, p-ERK and CD31 (at a dilution of 1:300,1:200 and 1:400 respectively) at 4°C overnight, followed by incubation with biotinylated polyclonal rabbit anti-rat antibody (1:200) in a humidified chamber for 1h. Positive reaction was observed with 3,3-diaminobenzidine as chromagen (DAB substrate kit; Vector Laboratories). The sections were counterstained with hematoxylin. Vessel density was determined by counting the number of microvessels per highpower field in the section. At least three fields were counted per animal and the average was taken as the microvessel density.

*Observation of potential toxicity*

The toxicities of treatment regimens were evaluated. Tissues of heart, liver, spleen, lung, kidney and brain were

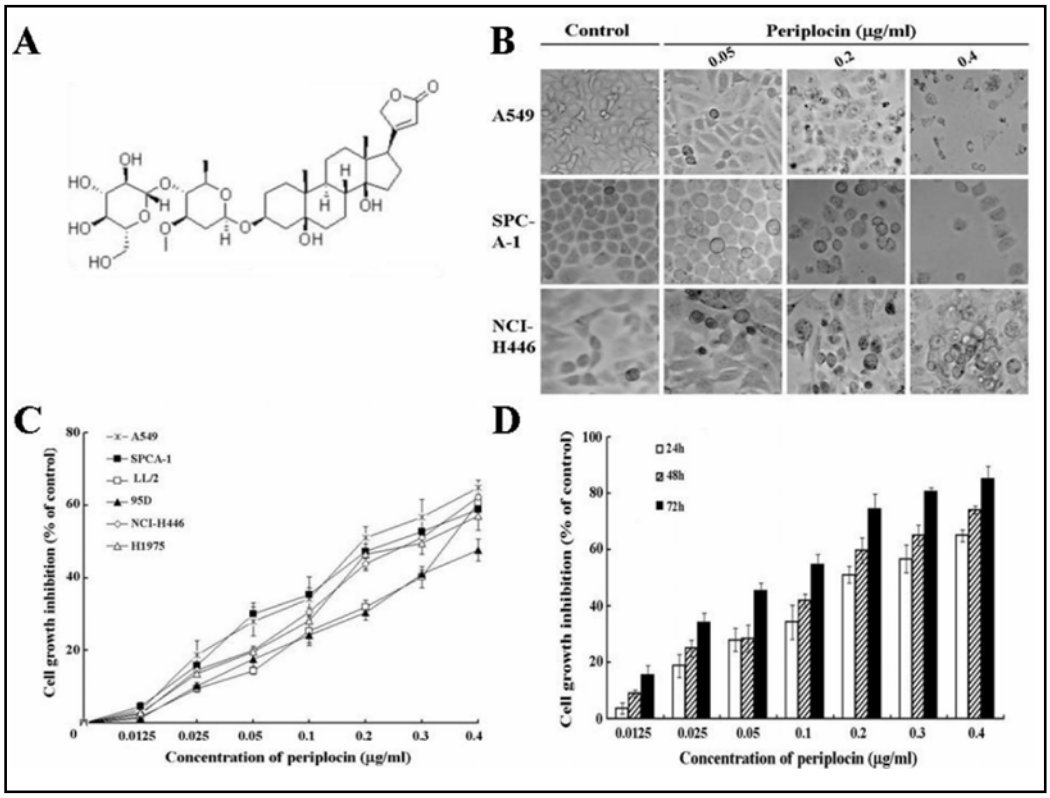


**Fig. 1.** (A) Structure of periplocin. (B) Representative morphological changes of A549, SPCA-1, and NCI-H446 cells treated with periplocin at different concentrations for 24 h. (C) Periplocin-inhibited proliferation of lung cancer cells in a dose-dependent manner. (D) Periplocin-inhibited proliferation of lung cancer cells in a time-dependent manner. Results of MTT assays are expressed as mean ± SD of 6 wells in triplicate experiments.

fixed in 10% formalin and embedded in paraffin. Sections of 4 μm were stained with H&E.

*Statistical analysis*

Data were expressed as mean ± SD. Statistical Package for the Social Science (SPSS) version 16.0 (Chicago, Illinois, USA) was used for statistical analysis. For comparison of a condition at individual time points, differences between the groups were tested by performing analysis of variance (ANOVA) and an unpaired Student t test. Survival curves were constructed according to the Kaplan-Meier method and statistical significance was determined by the log-rank test. Differences were considered significant at $P<0.05$.

## Results

*Inhibition of cell proliferation by periplocin*

The structure of periplocin is shown in Figure 1A. Nine subtypes of lung cancer cell lines mentioned above were employed to evaluate the inhibitory effects of periplocin. After treatment with periplocin for 48 h, the $IC_{50}$s of periplocin to A549, SPCA-1, H1975, NCI-H446, NCI-H460, NCI-H292, NCI-H69, 95D and LL/2 were approximately 0.08, 0.24, 0.21, 0.18, 0.4, 25, 37, 0.43 and 0.35μg/ml respectively (Table 1). Periplocin showed a dose- and time-dependent inhibitory effect on the growth of lung cancer cells. After treated with periplocin for 24, 48 and 72h, the growth of A549 cells was inhibited in a time-dependent manner (Figure1D). Additionally, as shown in Figure 1C, the inhibitory rates of 0.4 μg/ml periplocin against A549, SPCA-1, LL/2, 95D, NCI-H446 and H1975 were 65%, 59%, 60%, 48%, 62% and 57% respectively as compared with the control after treatment for 24 h.

*Periplocin-induced cell apoptosis and cell cycle arrest in vitro*

Flow cytometry and DNA Ladder were performed to investigate whether periplocin induced lung cancer cell apoptosis. The quantitative assessment of sub-G1 cells by flow cytometry was used to estimate the number of apoptotic cells. As shown in Figure 2A, periplocin increased the number of sub-G1 cells as compared with the control groups. Periplocin also promoted apoptosis of H1975, 95D, NCI-H460 and NCI-H446 cells. However, the pro-apoptotic effect of periplocin against NCI-H69 and NCI-H292 cells was not obvious (Table 2). Furthermore, agarose gel electrophoresis of periplocin-treated A549 cells demonstrated a ladder-like pattern of DNA fragments consisting of multiples of approximately 180-200 base pairs, consistent with internucleosomal DNA fragmentation (Figure 3).

Flow cytometry was employed to detect the effect of periplocin on cell cycle distribution. As shown in Figure 2B, periplocin resulted in significant accumulation of cells in G0/G1 phases in a dose-dependent manner, which was accompanied by a decrease in S DNA content, but not in

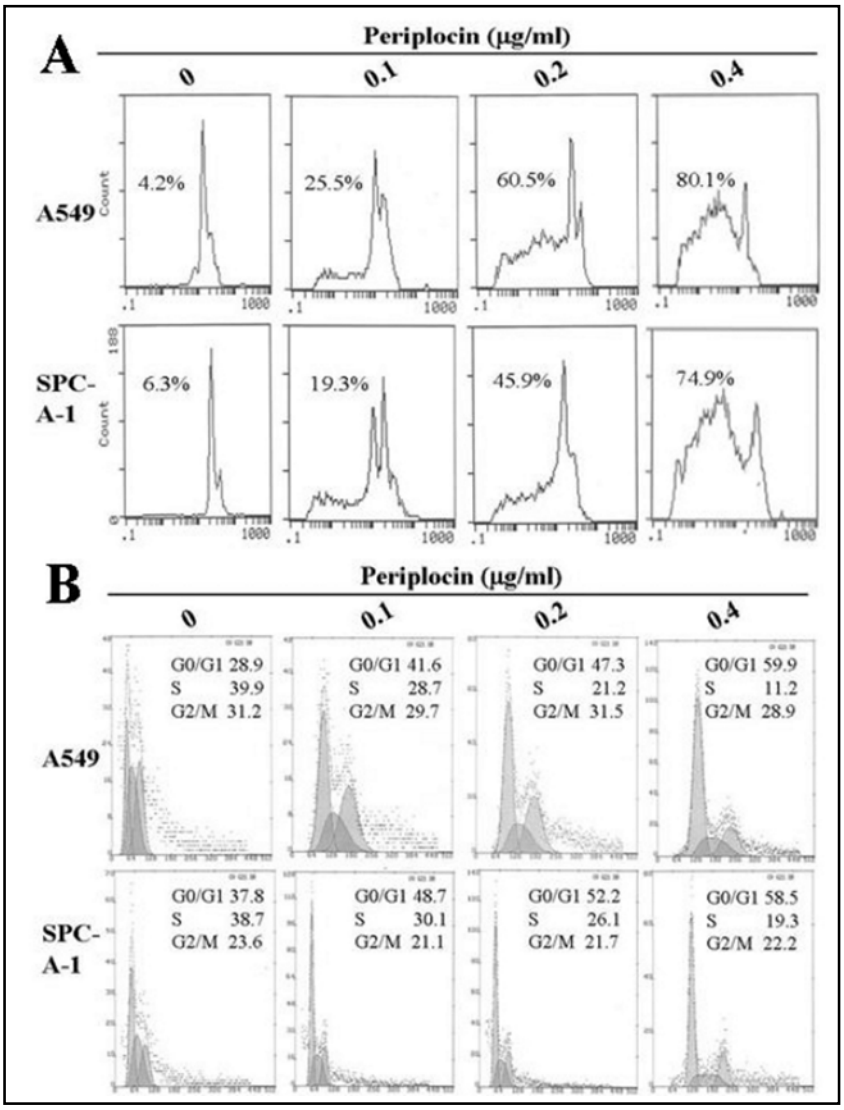


**Fig. 2.** Effects of periplocin on apoptosis and cell cycle distribution. Representative DNA fluorescence histograms of PI-stained cells. (A) After treated by periplocin at different concentrations for 48 h, apoptotic A549 and SPCA-1 cells were assessed by Flow cytometry. (B) Periplocin caused G0/G1 arrest in the cell cycle in A549 and SPCA-1 cells in a concentration-dependent manner after cells treated for 24 h.

G2/M. In addition, we performed FACS analysis of propidium iodide stained H1975, 95D, NCI-H460, NCI-H292, NCI-H446, NCI-H69 cells. We found that periplocin also reduces S phase and increases G0/G1 percentages in H1975 cells, however, the difference between cell cycle distribution in other cell lines was not significant.

*Antitumor efficacy of periplocin in vivo*

The established A549 and LL/2 tumor models were used to observe the effect of periplocin on the tumor burden of mice. The treatment regimens were performed as described in Materials and Methods. As shown in Figure 4B and C, compared with the control group, the periplocin-treated group demonstrated significant inhibition of tumor growth. For athymic nude mice, tumor volume of control group and treated group was (2363.25±255.38 $mm^3$) VS (729.72±97.76 $mm^3$) on day 29 and the data was (3075.95±403.71 $mm^3$) and (1230.12±193.41 $mm^3$) on day 40 for C57BL/6 mice. Three other groups of C57BL/6 mice (n=10 mice/group) were used to examine the life-prolonging effect of periplocin (Figure 4D). All untreated mice died of tumor burden within 33 days after implantation. The group that received 50μg of periplocin

| Tumor cell line | Apoptosis rate(%) | | | |
|---|---|---|---|---|
| | 0 | 0.1 | 0.2 | 0.4 (μ g/ml) |
| H1975 | 7.6 | 28.5 | 39.2 | 70.4 |
| 95D | 10.5 | 22 | 36.2 | 57.8 |
| NCI-H69 | 10.3 | 16.8 | 25.8 | 23.6 |
| NCI-H460 | 8.7 | 25.7 | 36.7 | 61.3 |
| NCI-H292 | 11.2 | 28.4 | 25.8 | 25.3 |
| NCI-H446 | 8.1 | 23.6 | 51.4 | 69.8 |

**Table 2.** The apoptosis rate in H1975, 95D, NCI-H460, NCI-H292, NCI-H446 and NCI-H69 cells treated by periplocin at different concentrations for 48 h.

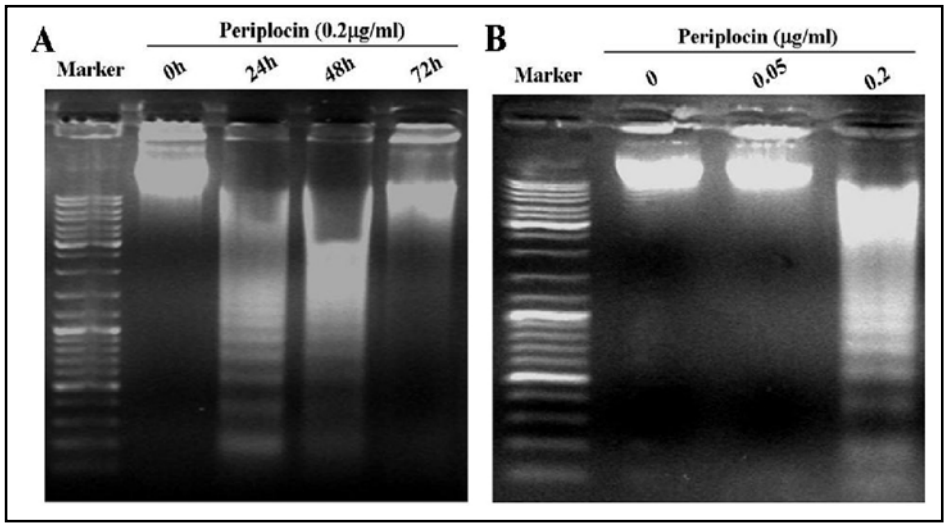


**Fig. 3.** Apoptosis of lung cancer cells induced by periplocin. (A) Agarose gel electrophoresis of DNA extracted from A549 cells treated by 0.2μg/mlperiplocin for 24, 48 and 72h respectively. (B) Agarose gel electrophoresis of DNA extracted from A549 cells treated with various concentrations of periplocin for 48 h.

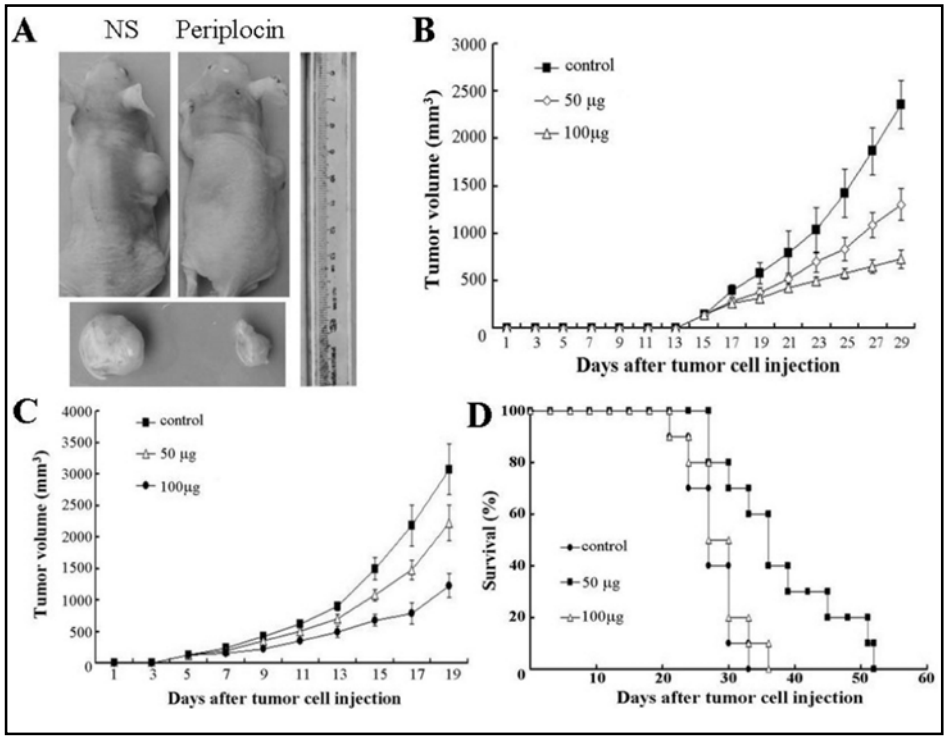


**Fig. 4.** Periplocin mediated inhibition of tumor growth. Mice were treated i.p. with with NS, periplocin(50μg) or periplocin(100μg) every day for 14 days. (A) Two representative athymic nude mice from NS-treated and periplocin(100μg)-treated groups were shown. (B) Antitumor efficacy of periplocin in the A549 model (n=5). (C) Antitumor efficacy of periplocin in the LL/2 model (n=10). The results were expressed by the mean volume ± SD. (D) Life-prolonging effect was determined by the survival time of LL/2 tumor-bearing mice(n=10).

showed a significantly prolonged survival time. However, enhanced survival rate was not observed in the groups treated with 100μg of periplocin, which demonstrated the potential toxicity of periplocin.

*Anti-angiogenesis and toxicity of periplocin*

The effect of periplocin on tumor angiogenesis was determined by immunolabeling CD31 in tissue sections. As shown in Figure 5, compared with the control group, the periplocin-treated groups showed a decreased microvessel density ($p<0.05$). Although the lack of survival increase in the periplocin(100μg)-treated mice was probably due to toxicity, obvious pathological changes in liver, kidney, lung and heart were not found in the HE-stained sections (Figure 6).

*Effect of periplocin on AKT, ERK and STAT3 signaling pathways*

To evaluate the role of periplocin on the critical growth and survival signaling pathways, such as AKT , ERK and STAT3, we exposed lung cancer cells to periplocin at different concentrations and analyzed phosphorylation of AKT , ERK and STAT3. As shown in Figure 7A, periplocin significantly blocked AKT and ERK phosphorylation in A549 cells compared with the controls, but not STAT3. *In vivo,* periplocin also decreased the phosphorylation levels of AKT and ERK (Figure 8). Moreover, periplocin eliminated the phosphorylation levels

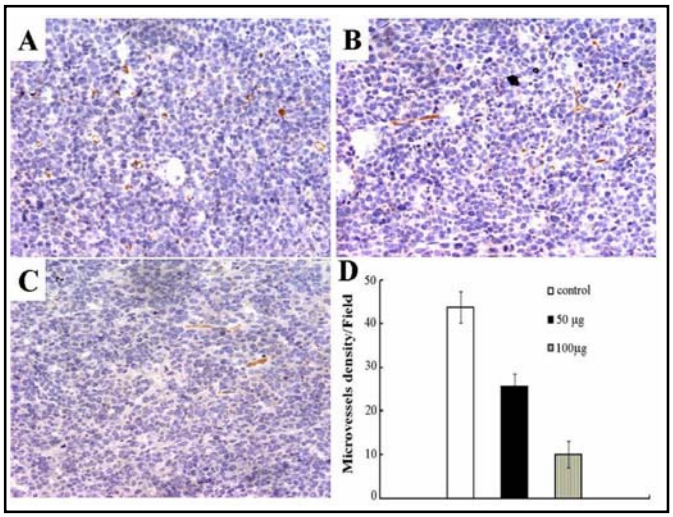


**Fig. 5.** Anti-angiogenesis activity of periplocin was evaluated by immunohistochemical assay. Vessel density was determined by counting the number of microvessels per high-power field in the sections stained with an antibody reactive to CD31, as described in Materials and Methods. (A) NS. (B) 50μg of periplocin. (C) 100μg of periplocin. (D) The average vessel density of three animals in each group was analyzed. Column, means; bars, ±SD.

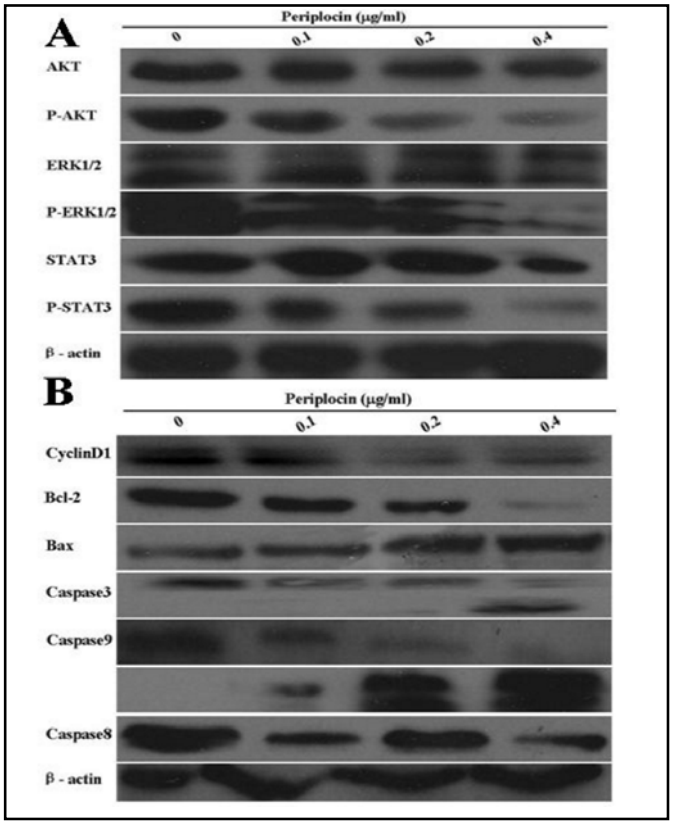


**Fig. 7.** Western blot analysis of A549 cells treated with periplocin. (A) A549 cells were treated with periplocin at various concentrations for 24 h. Periplocin eliminated the phosphorylation levels of Akt and ERK. (B) Cyclin D1 and Bcl-2 were inhibited. Apoptosis is also indicated by the induction of Bax, cleaved caspase-9 and caspase-3.

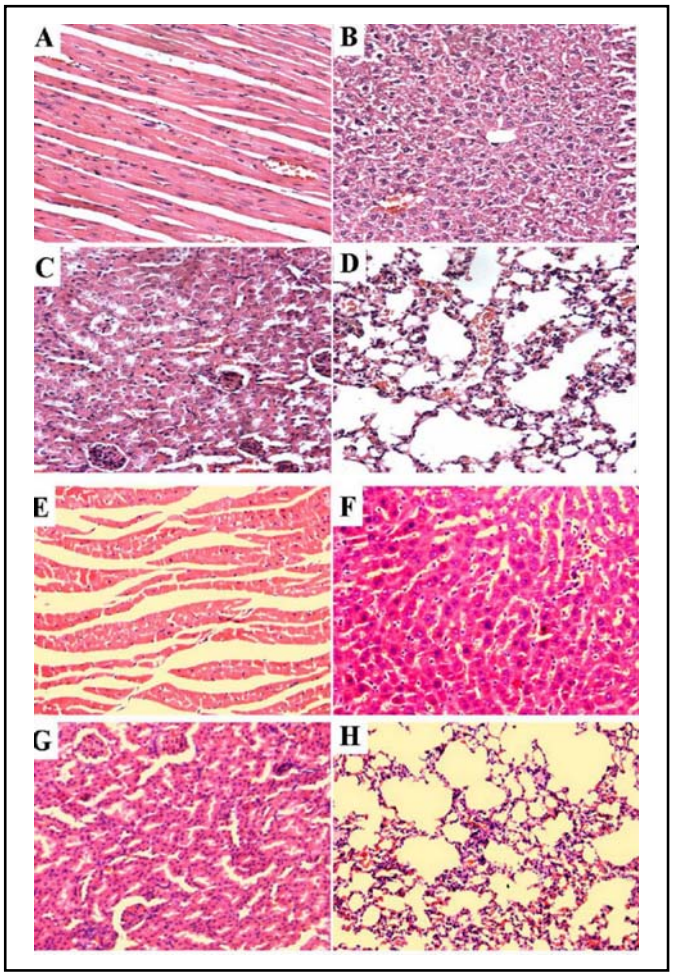


**Fig. 6.** Micrographs of hematoxylin/eosin-stained sections of heart, liver, kidney and lung. Internal organs from 100μg periplocin-treated (A-D) and controled (E-H) mice. Obvious pathological changes were not found.

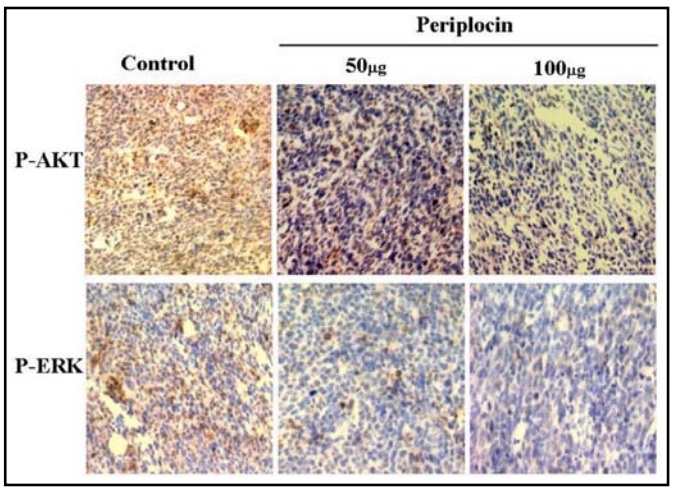


**Fig. 8.** Immunohistochemical staining for P-Akt and P-ERK in tumor tissues from controled, 50μg periplocin-treated and 100μg periplocin-treated C57BL/6 mice. Phosphorylated levels of AKT and ERK were decreased by periplocin.

of AKT and ERK in dose-dependent manners, but had no effect on the total levels of STAT3, AKT and ERK.

*Effect of periplocin on expression of cyclin D1, Bcl-2 and Bax*

Cyclin D1 plays a critical role in promoting the G1/S transition in the cell cycle and is often overexpressed in a variety of cancers. Loss of cyclin D1 can cause G1 arrest in cells [15]. In our study, cyclin D1 was downregulated by periplocin, which resulted in G0/G1 arrest in A549 cells (Figure 7B).

Members of the Bcl-2 family proteins function as gatekeepers of the cell death process. The proapoptotic Bcl-2 proteins such as Bax induce activation of caspase cascade for execution of the death program. The antiapoptotic Bcl-2 proteins such as Bcl-2 inhibit the function of proapoptotic Bcl-2 proteins [16]. To gain insights into the mechanism of apoptosis induced by periplocin, levels of Bcl-2 and Bax were determined by Western blot. As can be seen in Figure 7B, Bcl-2 protein level was significantly reduced, whereas Bax was activated in A549 cells treated with periplocin at various concentrations for 48 h. The results demonstrated that both Bax activation and Bcl-2 inhibition are required for the apoptosis inducd by periplocin.

*Involvement of caspases in periplocin-induced apoptosis*

Caspases are aspartate-specific cysteine proteases that play central roles in apoptosis processes [17]. As shown in Figure 7B, we explored effect of periplocin on activation of caspases by Western blot. Treatment of A549 cells with periplocin for 48 h resulted in cleavage of caspase-3 as evidenced by appearance of 19 kDa intermediate. Caspase-3 is an executioner caspase that can be activated by (a) mitochondrial pathway involving caspase-9 (intrinsic pathways) or (b) death receptor pathway involving caspase-8 (extrinsic pathways). Treatment of A549 cells with periplocin at different concentrations resulted in a significantly decreased level of procaspase-9, accompanied by increased cleaved caspase-9. The results suggested that periplocin triggered apoptosis through intrinsic pathway.

## Discussion

Accumulating preclinical and clinical data suggest that the cardiac glycosides have excellent activity against a variety of human solid tumor [6, 7]. Periplocin, one of the cardiac glycosides, was derived from cortex periplocae mainly used for treatment of rheumatoid arthritis, reinforcement of bones and tendons and alleviation of ache in lumbus and knee. Up to now, no information has been acquired concerning the anti-cancer effectiveness of periplocin for lung cancer *in vivo*. In the present study, we found that periplocin could inhibit the growth of lung cancer both *in vitro* and *in vivo*, which was associated with the inhibition of proliferation and the induction of apoptosis signaling pathway.

The cytotoxic activity of periplocin against nine subtypes of lung cancer cell lines was evaluated by MTT assay. After treatment with periplocin (0 to 0.4μg/ml) for 24, 48 and 72 h, the viability of lung cancer cells was obviously inhibited except for NCI-H292 and NCI-H69. Moreover, the inhibitory effect of periplocin on lung carcinoma cells was at a nanomolar level.

Apoptosis, induced by chemotherapy, radiation and cytokines, seems to be the main mechanism to kill tumor cells. To determine the anti-cancer mechanisms of periplocin, the proteins involved in cell proliferation and apoptosis were analyzed by Western blot. As the important signaling molecules, both AKT and ERK are upregulated in cancer cells and can phosphorylate series of transcription factors regulating gene expression, which is critical for cell proliferation, differentiation and survival [11, 12]. Activated AKT protects tumor cells from apoptosis through various stresses via multiple mechanisms, such as the phosphorylation of Bad, glycogen synthase-3, forkhead transcription factor and caspase-9 [18]. ERK can upregulate the expression of antiapoptotic proteins Bcl-2 and Bcl-xL by activating p90RSK [19]. Bcl-2/Bcl-xL may function by binding and sequestering Apaf-I, thus preventing apoptosome formation and subsequent caspase activation [16]. In our study, phosphorylated levels of AKT and ERK were significantly decreased by periplocin both *in vitro* and *in vivo*, which contributed to decreased angiogenesis and enhanced survival rate in the mice treated with periplocin. In addition, constitutive STAT3 signaling is involved in oncogenesis by mediating immune evasion and conferring resistance to apoptosis induced by conventional therapies [13]. However, periplocin had not obvious effect on the level of total STAT3 and P-STAT3, which demonstrated STAT3 signaling pathways was not inhibited by periplocin.

Apoptosis was a prominent factor in periplocin-induced growth inhibition, and the drug is also capable of promoting arrest at the G0/G1 phase of the cell cycle in A549 and SPCA-1 cells (Figure 2B). It was reported

periplocin increases S phase and reduces G0/G1 percentages in previously research [14]. The disparation could be explained from the different tumor cell lines and the decreased cyclin D1, moreover, our results were concordant with other studies [20]. In general, caspase activation in apoptosis occurs via two distinct pathways. One is the extrinsic pathway involving the death receptor signaling, and the other is the intrinsic pathway involving the mitochondrial cascades [21]. As the point-of-no-return in the apoptotic signaling cascade, caspase-3 activation is involved in either of the two pathways [22]. Caspase-3 and caspase-9, but not caspase-8, were activated by periplocin in our study, which indicated apoptosis was induced by periplocin through the intrinsic pathway. In addition, characteristic changes of apoptotic lung cancer cells were found, such as cell shrinkage, the condensation of chromatin in nucleus, and the digestion of chromatin into DNA fragments with lengths that multipled about 180 bp. Bcl-2 family members are critical regulators in the apoptosis cascade. The family members include antiapoptotic proteins such as Bcl-2 and Bcl-xL and proapoptotic members such as Bad, Bid, Bak and Bax [16]. As the major members of Bcl-2 family, Bcl-2 was downregulated, whereas Bax was upregulated in cells treated with periplocin.

*In vivo*, the signaling pathways elicited by the interaction of cardenolide with the sodium pump include modifications to the Src kinase, EGFR, Ras and ERK, all of which are associated with the biological behavior of lung cancer [23, 24]. Previous studies have shown that cardenolides, including digitoxin, oleandrin, ouabain, and UNBS1450, display antitumor effects on lung cancers both *in vitro* and *in vivo* by increasing $Ca^{2+}$ uptake, sustaining ROS production, initiating Apo2L/TRAIL apoptosis, decreasing phosphorylation of AKT, decreasing Hsp70, and blocking activation of NF-κB signaling pathway [25]. Here, our data suggested that periplocin, another cardiac glycoside, exhibited antitumor activity both in human and mouse lung cancer xenograft models by inhibiting AKT/ERK signaling pathways, downregulating cyclin D1 and Bcl-2, and increasing expression of Bax.

Taken together, on the basis of our findings *in vitro* and *in vivo*, treatment with periplocin produces both antiproliferative and proapoptotic effects. Moreover, judging from the constitutively activated AKT and ERK in many types of cancer, periplocin has the potential to be a therapeutic agent for the treatment of human lung caner, breast cancer, and so on. However, enhanced survival rate was not observed in the mice treated with 100μg of periplocin, which exhibited the potential toxicity. Therefore, periplocin deserves further exploration for its use as a potential agent in the therapy for cancer.

## Acknowledgements

This study was supported by the National Natural Science Foundation of China (No. 30872742).

## References

1 Jemal A, Siegel R, Ward E, Hao Y, Xu J, Thun MJ: Cancer statistics, 2009. CA Cancer J Clin 2009;59:225-249.

2 Rajeswaran A, Trojan A, Burnand B, Giannelli M: Efficacy and side effects of cisplatin- and carboplatin-based doublet chemotherapeutic regimens versus non-platinum-based doublet chemo-therapeutic regimens as first line treatment of metastatic non-small cell lung carcinoma: a systematic review of randomized controlled trials. Lung Cancer 2008;59:1-11.

3 Efferth T, Li PC, Konkimalla VS, Kaina B: From traditional Chinese medicine to rational cancer therapy. Trends Mol Med 2007;13:353-361.

4 Mijatovic T, Van Quaquebeke E, Delest B, Debeir O, Darro F, Kiss R: Cardiotonic steroids on the road to anti-cancer therapy.Biochim Biophys Acta 2007;1776:32-57.

5 Winnicka K, Bielawski K, Bielawska A, Surazyñski A: Antiproliferative activity of derivatives of ouabain, digoxin and proscillaridin A in human MCF-7 and MDA-MB-231 breast cancer cells. Biol Pharm Bull 2008;31:1131-1140.

6 Mekhail T, Kaur H, Ganapathi R, Budd GT, Elson P, Bukowski RM: Phase 1 trial of Anvirzel in patients with refractory solid tumors.Invest New Drugs 2006;24:423-427.

7 Schoner W, Scheiner-Bobis G: Endogenous and exogenous cardiac glycosides: their roles in hypertension, salt metabolism, and cell growth. Am J Physiol Cell Physiol 2007;293:C509-536.

8 Okada H, Mak TW: Pathways of apoptotic and non-apoptotic death in tumour cells. Nat Rev Cancer 2004;4:592-603.

9 Singh R, George J, Shukla Y: Role of senescence and mitotic catastrophe in cancer therapy. Cell Div 2010;5:4.
10 Mathieu A, Remmelink M, D'Haene N, Penant S, Gaussin JF, Van Ginckel R, Darro F, Kiss R, Salmon I: Development of a chemoresistant orthotopic human nonsmall cell lung carcinoma model in nude mice: analyses of tumor heterogenity in relation to the immunohistochemical levels of expression of cyclooxygenase-2, ornithine decarboxylase, lung-related resistance protein, prostaglandin E synthetase, and glutathione-S-transferase-alpha (GST)-alpha, GST-mu, and GST-pi. Cancer 2004;101:1908-1918.
11 Vicent S, López-Picazo JM, Toledo G, Lozano MD, Torre W, Garcia-Corchón C: ERK1/2 is activated in non-small-cell lung cancer and associated with advanced tumours. Br J Cancer 2004;90:1047-1052.
12 Balsara BR, Pei J, Mitsuuchi Y, Page R, Klein-Szanto A, Wang H: Frequent activation of AKT in non-small cell lung carcinomas and preneoplastic bronchial lesions. Carcinogenesis 2004;25:2053-2059.
13 Alvarez JV, Febbo PG, Ramaswamy S, Loda M, Richardson A, Frank DA: Identification of a genetic signature of activated signal transducer and activator of transcription 3 in human tumors. Cancer Res 2005;65:5054-5062.
14 Bloise E, Braca A, De Tommasi N, Belisario MA: Pro-apoptotic and cytostatic activity of naturally occurring cardenolides. Cancer Chemother Pharmacol 2009;64:793-802.
15 Masamha CP, Benbrook DM: Cyclin D1 degradation is sufficient to induce G1 cell cycle arrest despite constitutive expression of cyclin E2 in ovarian cancer cells. Cancer Res 2009;69:6565-6572.
16 Autret A, Martin SJ: Emerging role for members of the Bcl-2 family in mitochondrial morphogenesis. Mol Cell 2009;36:355-363.
17 Brenner D, Mak TW: Mitochondrial cell death effectors. Curr Opin Cell Biol 2009;21:871-877.
18 Toker A, Yoeli-Lerner M: Akt signaling and cancer: surviving but not moving on. Cancer Res 2006;66:3963-3966.
19 Anjum R, Blenis J: The RSK family of kinases: emerging roles in cellular signalling. Nat Rev Mol Cell Biol 2008;9:747-758.
20 Du YY, Liu X, Shan BE: Periplocin extracted from cortex periplocae induces apoptosis of SW480 cells through inhibiting the Wnt/beta-catenin signaling pathway. Ai Zheng 2009;28:456-460.
21 Fulda S: Apoptosis pathways and neuroblastoma therapy. Curr Pharm Des 2009;15:430-435.
22 Smith DJ, Ng H, Kluck RM, Nagley P: The mitochondrial gateway to cell death. IUBMB Life 2008;60:383-389.
23 Wang H, Haas M, Liang M, Cai T, Tian J, Li S, Xie Z: Ouabain assembles signaling cascades through the caveolar Na+/K+-ATPase. J Biol Chem 2004;279:17250-17259.
24 Janmaat ML, Rodriguez JA, Gallegos-Ruiz M, Kruyt FA, Giaccone G: Enhanced cytotoxicity induced by gefitinib and specific inhibitors of the Ras or phosphatidyl inositol-3 kinase pathways in non-small cell lung cancer cells. Int J Cancer 2006;118:209-214.
25 Newman RA, Yang P, Pawlus AD, Block KI: Cardiac glycosides as novel cancer therapeutic agents. Mol Interv 2008;8:36-49.